ISSN 1674-1056
http://cpb.iphy.ac.cn
http://iopscience.iop.org/cpb
中国物理 B
Chinese Physics
中国物理
Chinese Physics B

# Generation of diffraction-free vectorial elliptic hollow beams with space-varying inhomogeneous polarizations

Hui-Rong Li(李会容), Peng-Yi Zhao(赵朋义), and Jian-Ping Yin(印建平)
**Citation:**Chin. Phys. B, 2021, 30 (**8**): 084204. DOI: 10.1088/1674-1056/abe3e9
Journal homepage: http://cpb.iphy.ac.cn; http://iopscience.iop.org/cpb

**What follows is a list of articles you may be interested in**

---

## Generation of cavity-birefringence-dependent multi-wavelength bright-dark pulse pair in a figure-eight thulium-doped fiber laser

Xiao-Fa Wang(王小发), Dong-Xin Liu(刘东鑫), Hui-Hui Han(韩慧慧), and Hong-Yang Mao(毛红炀)
Chin. Phys. B, 2021, 30 (**5**): 054205. DOI: 10.1088/1674-1056/abd68f

## Generation of single and multiple dissipative soliton in an erbium-doped fiber laser

Li-Na Duan(段利娜), Jin Wen(文进), Wei Fan(樊伟), Wei Wang(王炜)
Chin. Phys. B, 2017, 26 (**10**): 104205. DOI: 10.1088/1674-1056/26/10/104205

## Passive polarization rotator based on silica photonic crystal fiber for 1.31-μm and 1.55-μm bands via adjusting the fiber length

Chen Lei, Zhang Wei-Gang, Wang Li, Bai Zhi-Yong, Zhang Shan-Shan, Wang Biao, Yan Tie-Yi, Jonathan Sieg
Chin. Phys. B, 2014, 23 (**10**): 104220. DOI: 10.1088/1674-1056/23/10/104220

## Nonlinear polarization rotation-induced pulse shaping in a stretched-pulse ytterbium-doped fiber laser

Bai Dong-Bi, Li Wen-Xue, Yang Kang-Wen, Shen Xu-Ling, Chen Xiu-Liang, Zeng He-Ping
Chin. Phys. B, 2014, 23 (**10**): 104208. DOI: 10.1088/1674-1056/23/10/104208

## An all-optical buffer based on polarization rotation in an EAM

Wang Kui-Ru, Kuang Hai, Wang Yong-Jun, Yuan Jin-Hui, Yan Bin-Bin
Chin. Phys. B, 2013, 22 (**8**): 084201. DOI: 10.1088/1674-1056/22/8/084201

---

# Generation of diffraction-free vectorial elliptic hollow beams with space-varying inhomogeneous polarizations*

Hui-Rong Li(李会容)[1,†], Peng-Yi Zhao(赵朋义)[1], and Jian-Ping Yin(印建平)[2]

[1] College of Physics and Electronic Science, Hubei Normal University, Huangshi 435002, China
[2] State Key Laboratory of Precision Spectroscopy, East China Normal University, Shanghai 200062, China

(Received 16 January 2021; revised manuscript received 3 February 2021; accepted manuscript online 7 February 2021)

Diffraction-free vectorial elliptic hollow beams (vEHBs) are generated by an optical system composed of a short elliptic hollow fiber (EHF) and an axicon. Each beam has a closed elliptic annular intensity profile and space-varying polarization states in its diffraction-free distance of more than 1 m. The generated beams have a counter-clockwise or clockwise periodically-rotated inhomogeneous polarization. And the spin angular momentum (SAM) of the vEHBs is $1\hbar$ or $-1\hbar$ which is consistent with the type of dual-mode in the EHF and the periodic polarization rotations of the vEHBs. The vEHBs have potential applications in optically trapping and micromanipulating the micro- or nano-particles, quantum information transmission, and Bose–Einstein condensates, *etc*.

**Keywords:** elliptic hollow beam, vectorial beam, polarization rotation

**PACS:** 42.81.–I, 42.15.–i **DOI:** 10.1088/1674-1056/abe3e9

## 1. Introduction

Vectorial beams have potential applications in optically trapping and micromanipulating the micro- or nano-particles (including cold atoms or molecules),[1–3] quantum information processing and transmission, contrast enhancement in light microscopy, *etc*.[4] In optical communication, the properties of a light beam, such as its intensity, wavelength, polarization, and orbital angular momentum, can be used to increase the channel capacity to efficiently transmit the information.[5] And new dynamical characteristics will emerge in the elliptic symmetric electromagnetic field.[6] Although radially and azimuthally polarized diffraction-free fields[7] and diffraction-free Bessel beams with space-varying polarizations have been generated,[8] vectorial elliptic hollow beams with space-varying polarizations are difficult to produce, which has limited possibilities for experimental studies.

We will present a practical scheme to produce a series of vectorial diffraction-free elliptic hollow beams with space-varying polarizations in this paper. We have reported that the dual-mode composed of ${}_{\rm e}{\rm HE}_{11}$ mode and ${}_{\rm o}{\rm HE}_{11}$ mode in the elliptic hollow fiber (EHF) can be used to generate a self-focusing vectorial elliptic hollow beam (vEHB), which finally becomes a vectorial Mathieu-like hollow beam by passing through an axicon optical system.[9] In fact, when a focused Gaussian beam is coupled into the core of an EHF, variant modes can be selectively excited with variant suitable incident angles, and another dual-mode waveguide (composed of ${}_{\rm e}{\rm HE}_{1n}$ mode and ${}_{\rm o}{\rm HE}_{1n}$ mode, $n > 1$) can be formed in the EHF. According to our earlier research, the intensity profiles of ${}_{\rm e}{\rm HE}_{1n}$ modes ($n = 1, 2, 3, 4, 5, 6$) are closed elliptic rings as shown in Fig. 1, and the ${}_{\rm o}{\rm HE}_{1n}$ mode has a similar elliptic annular intensity profile to the corresponding ${}_{\rm e}{\rm HE}_{1n}$ mode.[10] Figure 1 also shows that the ${}_{\rm e}{\rm HE}_{1n}$ mode and ${}_{\rm o}{\rm HE}_{1n}$ mode with odd $n$ have their maximum intensities in the $y$ direction, and the ${}_{\rm e}{\rm HE}_{1n}$ mode and ${}_{\rm o}{\rm HE}_{1n}$ mode with even $n$ have their maximum intensities in the $x$ direction. Therefore, we can selectively excite another dual-mode (composed of ${}_{\rm e}{\rm HE}_{1n}$ mode and ${}_{\rm o}{\rm HE}_{1n}$ mode, with $n > 1$) and guide this dual-mode in the EHF, let it output from the EHF and pass through the axicon optical system to obtain a vEHB. The vEHBs generated by other dual-modes may have some different properties.

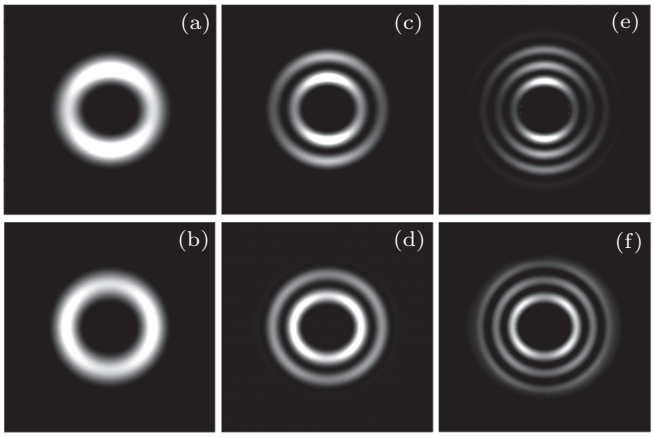



**Fig. 1.** Transverse intensity profiles of (a) ${}_{\rm e}{\rm HE}_{11}$, (b) ${}_{\rm e}{\rm HE}_{12}$, (c) ${}_{\rm e}{\rm HE}_{13}$, (d) ${}_{\rm e}{\rm HE}_{14}$, (e) ${}_{\rm e}{\rm HE}_{15}$, and (f) ${}_{\rm e}{\rm HE}_{16}$ modes, with each panel being 30 μm×30 μm in size.[10]

In this paper, we will present some different properties of

*Project supported by the National Natural Science Foundation of China (Grant Nos. 11304093 and 11274114), the Hubei Provincial Natural Science Foundation, China (Grant No. 2018CFB320), and the Academic Discipline Project of Hubei Normal University, China (Grant Nos. 2014F012 and 2014F013).

†Corresponding author. E-mail: lhr-2000@163.com

© 2021 Chinese Physical Society and IOP Publishing Ltd 

the vEHBs generated by other dual-modes. The rest of this paper is organized as follows. In Section 2, we give the scheme to produce the vEHBs by using an optical system composed of a short dual-mode EHF and an axicon. In Section 3, we describe the longitudinal and transverse propagation properties of the vEHBs, and obtain the diffraction-free region of each vEHB. And in Section 4, we obtain the polarization states and spin angular momentum (SAM) of the diffraction-free vEHBs generated by different dual-modes in the EHF and its propagation evolutions. In Section 5, we draw some conclusions from our present study.

## 2. Scheme to generate vectorial elliptic hollow beams

The optical system composed of an EHF and an axicon to produce some vEHBs is shown in Fig. 2. The EHF has three layers: the hollow region, the core, and the cladding. In our scheme, a focused Gaussian beam is coupled into the core of the EHF with a suitable incident angle to selectively excite another dual-mode ($_{e}HE_{1n}$ mode and $_{o}HE_{1n}$ mode, with $n > 1$). The excited dual-mode is diffracted by the outlet of the EHF, and output as an elliptic hollow beam (EHB), which has a weak first-order and a few weaker high-order diffraction rings around the zero-order diffraction ring. We use an aperture to filter the diffracted beam to obtain the zero-order diffraction ring, and two positive lenses with different focal lengths to expand and reshape the zero-order diffractive EHB. Finally, we let the resulting EHB illuminate the axicon to generate an approximate diffraction-free vEHB in the darker shaded region in Fig. 2.

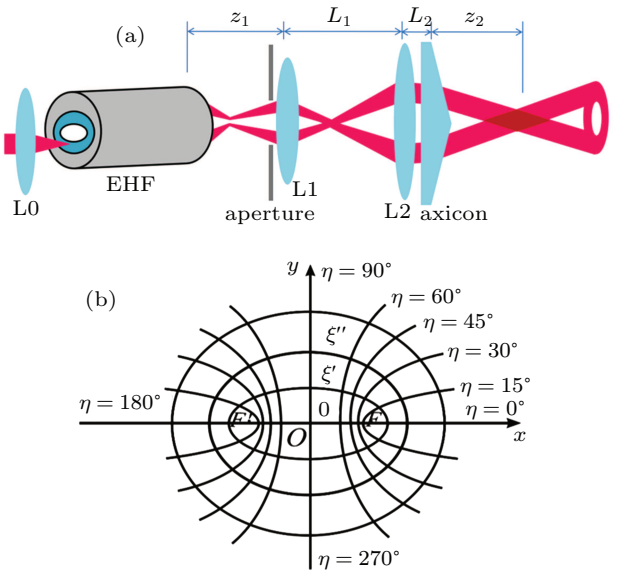



**Fig. 2.** (a) Generation scheme of vEHBs,[9] and (b) elliptic coordinate system.

The EHF is placed along the $z$ direction, and the long axis of the elliptic cross section is in the $x$ direction. The refractive indices of its three layers are $n_0 = 1$, $n_1 = 1.4530$, and $n_2 = 1.4502$, respectively. We utilize the orthogonal elliptic coordinate system $(\xi, \eta, z)$ [see Fig. 2(b)] to solve Maxwell's equations to obtain the dual-mode guided in the EHF.[9] And in the elliptic coordinate system, the inner boundary of the core of the EHF is located at $\xi' = 1.40$ with eccentricity $\tau = 0.46$, the outer boundary of the core is at $\xi'' = 2.40$, and the outer diameter of the cladding can be taken to be infinite.The half focal distance of the boundaries, $h$, is 3.25 μm. And the elliptic coordinates are defined in terms of Cartesian system by $x = h\cosh\xi\cos\eta$, $y = h\sinh\xi\sin\eta$, and $z = z$. We assume that the laser power coupled into the EHF is 0.5 W, and the constituents of the dual-mode in the EHF, $_{e}HE_{1n}$ mode and $_{o}HE_{1n}$ mode, have the same power, so each mode obtains the power of 0.25 W. The longitudinal and transverse electromagnetic fields of the dual-mode, $H_z$, $E_z$, $H_\xi$, $E_\xi$, $H_\eta$, and $E_\eta$, can be derived by a vectorial model based on Maxwell's equations, and their intensities can be calculated by the longitudinal component of the time-averaged Poynting vector $S_z = (1/2)\,\mathrm{Re}(E_\xi H_\eta^* - E_\eta H_\xi^*)$, which indicates a closed elliptic hollow ring.[10]

We set $z = 0$ at the outlet of the EHF, and the light beam diffracted from the EHF propagates along the $z$ axis. At the propagation distance $z_1$, the electromagnetic field distribution in free space can be calculated by the vectorial Rayleigh–Sommerfeld diffraction integral. The electric (magnetic) field components in the EHF and the fields at $z_1$ are denoted as $\tilde{E}_j(\xi, \eta, 0)$ and $\tilde{E}_j(\xi_1, \eta_1, z_1)$ respectively. Here $j = \xi, \eta$ or $z$.

The electromagnetic-field distribution of the output EHB passing through the axicon optical system can be calculated and analyzed by using the Collins formula[11]

$$\begin{aligned}
&\tilde{E}_j(\xi_2, \eta_2, z_1 + z_3) \\
&= \frac{-\mathrm{i}}{\lambda B}\int_0^{2\pi}\int_0^{\infty} \tilde{E}_j(\xi_1, \eta_1, z_1) \\
&\times \exp\left[\mathrm{i}kz_3 + \frac{\mathrm{i}k}{2B}\left(A\left(x_1^2 + y_1^2\right) - 2\left(x_1x_2 + y_1y_2\right)\right.\right. \\
&\left.\left. + D\left(x_2^2 + y_2^2\right)\right)\right] \\
&\times \exp\left[-k\alpha(n-1)h\sqrt{\sinh^2\xi_1 + \cos^2\eta_1}\right] \\
&\times h^2\left(\cosh^2\xi_1 - \cos^2\eta_1\right)\mathrm{d}\xi_1\mathrm{d}\eta_1,
\end{aligned} \tag{1}$$

where $z_3 = L_1 + L_2 + z_2$, and $\tilde{E}_j(\xi_2, \eta_2, z_1 + z_3)$ is the electric (magnetic) field component at $z_2$ plane after the axicon, and $x_1 = h\cosh\xi_1\cos\eta_1$, $y_1 = h\sinh\xi_1\sin\eta_1$, $x_2 = h\cosh\xi_2\cos\eta_2$, and $y_2 = h\sinh\xi_2\sin\eta_2$. The $A$, $B$, $C$, and $D$ are the elements of the following transfer matrix:

$$\begin{pmatrix} A & B \\ C & D \end{pmatrix} = \begin{pmatrix} 1-L_1/f_1+(L_2+z_2)(L_1-f_1-f_2)/f_1f_2 & L_2+z_2+L_1[1-(L_2+z_2)/f_2] \\ -(f_1+f_2-L_1)/f_1f_2 & 1-L_1/f_2 \end{pmatrix} \tag{2}$$

and $f_1$ and $f_2$ are the focal lengths of the two lenses (L1, L2) respectively, $L_1$ is the distance between the two positive lenses, and $L_2$ is the distance between the second lens and the axicon. The refractive index of the axicon is $n = 1.51$, the wedge angle of the axicon is $\alpha = 0.1°$, which can be fabricated by electron-beam lithography.[12] We first focus on the dual-modes of $n = 2$, 3, 5, respectively. We selectively excite a dual-mode composed of ${}_{\rm e}{\rm HE}_{12}$ mode and ${}_{\rm o}{\rm HE}_{12}$ mode in the core of the EHF, and assume that $f_1 = 0.5$ cm, $f_2 = 20$ cm, $L_1 = 19.3$ cm, $L_2 = 0.5$ cm, and $z_1 = 1$ cm. When a dual-mode composed of ${}_{\rm e}{\rm HE}_{13}$ mode and ${}_{\rm o}{\rm HE}_{13}$ mode is selectively excited, we have $f_1 = 0.5$ cm, $f_2 = 30$ cm, $L_1 = 29$ cm, $L_2 = 0.5$ cm, and $z_1 = 1$ cm. When the dual-mode excited in the core of the EHF is composed of ${}_{\rm e}{\rm HE}_{15}$ mode and ${}_{\rm o}{\rm HE}_{15}$ mode, we have $f_1 = 0.5$ cm, $f_2 = 50$ cm, $L_1 = 50$ cm, $L_2 = 0.5$ cm, and $z_1 = 1$ cm. We can obtain the light field distribution in the dark region after the axicon by carrying out some numerical calculations on the transformation of this *ABCD* optical system and the longitudinal component of the time-averaged Poynting vector.

## 3. Propagation and polarization properties of the diffraction-free EHBs

Figure 3 illustrates the longitudinal intensity distributions of the three diffraction-free EHBs generated by the three dual-modes with $n = 2$, 3, 5. The central elliptic ring of the diffraction-free EHB generated by the dual-mode of $n = 2$ (${}_{\rm e}{\rm HE}_{12}$ mode and ${}_{\rm o}{\rm HE}_{12}$ mode), keeps unchanged within a distance of 1.9 m. And the diffraction-free distance of the EHBs generated by the dual-mode of $n = 3$ (${}_{\rm e}{\rm HE}_{13}$ mode and ${}_{\rm o}{\rm HE}_{13}$ mode) and the dual-mode of $n = 5$ (${}_{\rm e}{\rm HE}_{15}$ mode and ${}_{\rm o}{\rm HE}_{15}$ mode), maintain 1.5 m and 2.5 m, respectively. In each panel of Fig. 3, it can be seen that the maximum intensity in $y$-axis direction varies with the propagation distance $z_2$.

Figure 4 exhibits the transverse intensity distributions of the diffraction-free EHBs ($n = 2$, 3, 5). Figures 4(a)–4(c) illustrate the transverse intensities of the diffraction-free EHB generated by the ${}_{\rm e}{\rm HE}_{12}$ mode and ${}_{\rm o}{\rm HE}_{12}$ mode at $z_2 = 2.0$ m, 2.9 m, and 3.8 m. Figures 4(d)–4(f) illustrate the transverse intensities of the beam generated by the ${}_{\rm e}{\rm HE}_{13}$ mode and ${}_{\rm o}{\rm HE}_{13}$ mode at $z_2 = 2.8$ m, 3.5 m, and 4.2 m. And the transverse intensities of the beam generated by the ${}_{\rm e}{\rm HE}_{15}$ mode and ${}_{\rm o}{\rm HE}_{15}$ mode at $z_2 = 5.7$ m, 7.2 m, and 7.8 m are shown in Figs. 4(g)–4(i). Each EHB has a propagation-unchanged elliptic ring in the center with a relative intensity change in the diffraction-free region, which can maintain several meters. Figure 4 also shows that the diffraction-free EHB generated by ${}_{\rm e}{\rm HE}_{12}$ mode and ${}_{\rm o}{\rm HE}_{12}$ mode have two maximum intensities in the $x$ direction in each $z_2$-plane; and the diffraction-free EHB generated by the ${}_{\rm e}{\rm HE}_{13}$ mode and ${}_{\rm o}{\rm HE}_{13}$ mode, and the diffraction-free EHBs generated by the ${}_{\rm e}{\rm HE}_{15}$ mode and the ${}_{\rm o}{\rm HE}_{15}$ mode have their maximum intensities in the $y$ direction in each $z_2$-plane. The arrows in Fig. 4 indicate that the three diffraction-free EHBs have inhomogeneous polarization states in their cross sections, *i.e.*, they are diffraction-free vEHBs, and the polarization directions of the diffraction-free vEHBs vary with propagation distance.

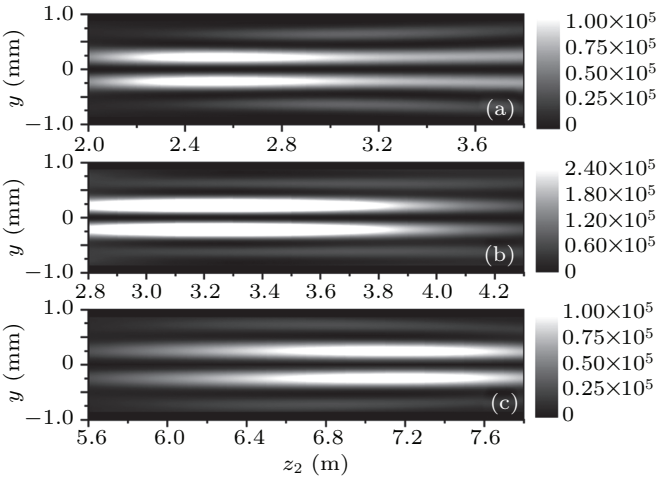



**Fig. 3.** Longitudinal intensity distributions of diffraction-free EHBs. $z_2$ is the distance after the axicon. Light beams are generated by three dual-modes with $n = 2$ (a), 3 (b), and 5 (c), respectively.

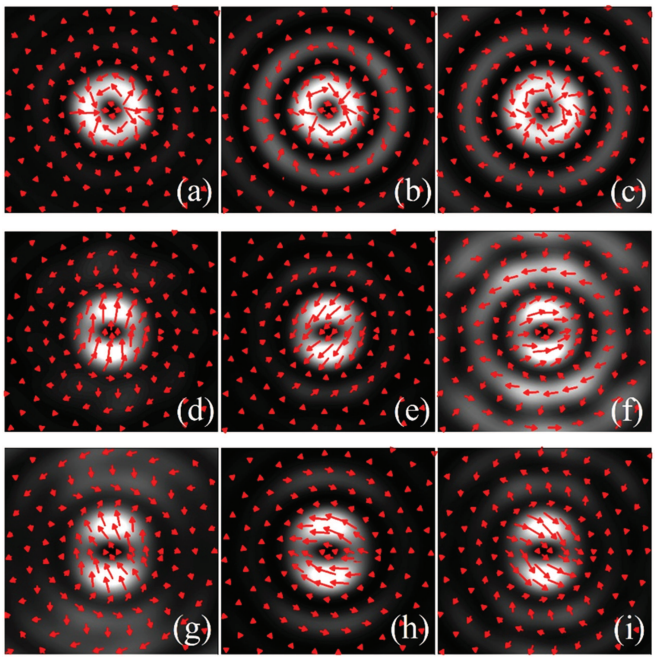



**Fig. 4.** Transverse intensity distributions in diffraction-free region, with bright area indicating relative intensity, arrow referring to polarization state of beam, and each panel being 1 mm×1 mm in size.

If a dual-mode composed of the ${}_{\rm e}{\rm HE}_{14}$ mode and the

$_{o}HE_{14}$ mode is selectively excited in the EHF, we set $f_1 = 0.5$ cm, $f_2 = 30$ cm, $z_1 = 1$ cm, $L_1 = 29.5$ cm, and $L_2 = 0.5$ cm to obtain a diffraction-free EHB with an unchanged propagation distance of 1.5 m. If a dual-mode composed of the $_{e}HE_{16}$ mode and the $_{o}HE_{16}$ mode is selectively excited, we set $f_1 = 0.5$ cm, $f_2 = 32$ cm, $z_1 = 1$ cm, $L_1 = 31.6$ cm, and $L_2 = 0.5$ cm to obtain a diffraction-free EHB with an unchanged propagation distance of 2 m. Our study shows that the diffraction-free EHBs generated by the six dual-modes ($n = 1$, 2, 3, 4, 5, 6) are diffraction-free vEHBs, and they have inhomogeneous polarization states in their cross sections and their polarization directions vary with propagation distance.

## 4. Polarization states and spin angular momentum of diffraction-free EHBs and their propagation properties

We further calculate in detail the polarization states of these vEHBs in their diffraction-free regions. Figure 5(a) shows the clockwise rotation and inhomogeneous polarization states of the vEHB generated by the dual-mode of the $_{e}HE_{12}$ mode and the $_{o}HE_{12}$ mode in the transverse plane at $z_2 = 3.0$ m. Figure 5(b) shows the counter-clockwise rotation and inhomogeneous polarization states of the vEHB generated by the $_{e}HE_{13}$ mode and the $_{o}HE_{13}$ mode at $z_2 = 3.5$ m. And figure 5(c) shows the counter-clockwise rotation and inhomogeneous polarization states of the vEHBs generated by the $_{e}HE_{15}$ mode and the $_{o}HE_{15}$ mode at $z_2 = 7.2$ m. The results of our calculation suggest that the diffraction-free vEHBs of $n = 4$ and 6 both have the similar clockwise rotations and inhomogeneous polarization states to the vEHBs generated by the dual-mode composed of the $_{e}HE_{12}$ mode and the $_{o}HE_{12}$ mode. To save the space, we do not present the intensity results or the polarization results of the diffraction-free vEHBs of $n = 4$ and 6.

Our calculation results also indicate that the polarization rotations of the diffraction-free vEHBs are periodically around the propagation axis, and they are counter-clockwise for the dual-modes of odd $n$ and clockwise for the dual-modes of even $n$. All these vEHBs have the same rotation period which equals the laser wavelength $\lambda$. As can be seen from Fig. 5, the polarization directions of the light beam in the two adjacent diffraction rings are almost opposite in each $z_2$-plane, and the polarization patterns of the vEHBs generated by the dual-mode of even $n$ ($_{e}HE_{12}$ and $_{o}HE_{12}$ mode) are quite different from those of the vEHBs of odd $n$.

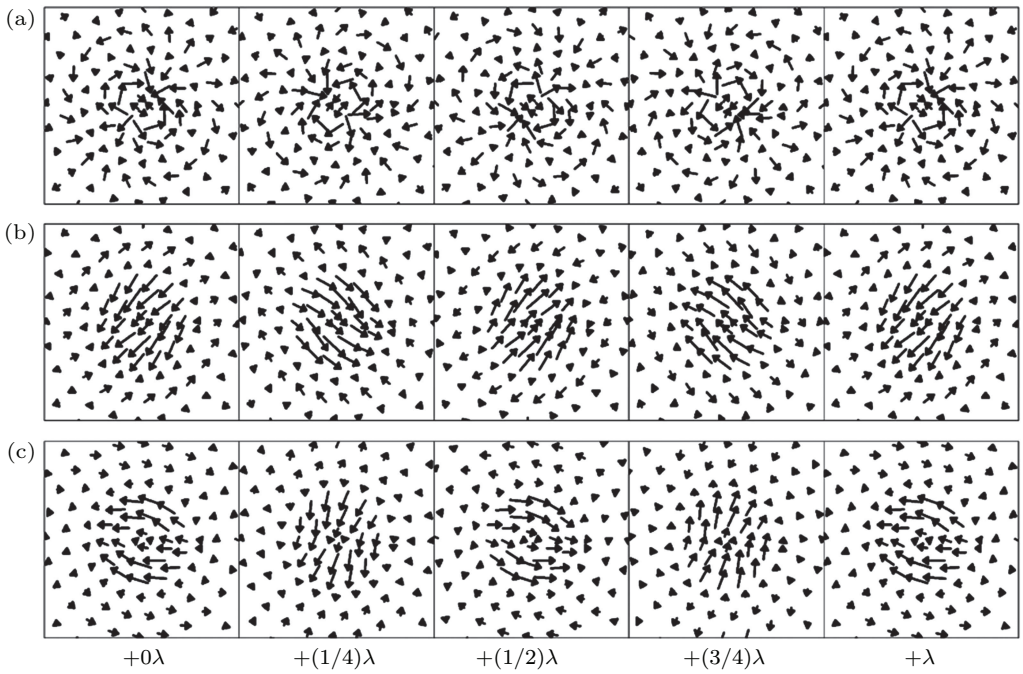



**Fig. 5.** Distributions of polarization states for diffraction-free vEHBs ($n = 2$, 3, 5), with arrows showing polarization states of beam in each $z_2$-plane.

The SAM can be calculated numerically from[10,13]

$$\delta J_{\mathrm{sp}} = \sigma\hbar = \frac{-\mathrm{i}\hbar\left(E_x E_y^* - E_y E_x^*\right)}{|E_x|^2 + |E_y|^2}. \tag{3}$$

The $E_\xi$ and $E_\eta$ are light field components in the elliptic coordinate system, and can be numerically calculated from Eq. (1). The $E_x$ and $E_y$ are light field components in the $x$ and $y$ directions in $z_2$ planes, and can be given by

$$E_x = \frac{\sinh\xi\cos\eta E_\xi - \cosh\xi\sin\eta E_\eta}{\sqrt{\sinh^2\xi + \sin^2\eta}}, \tag{4}$$

$$E_y = \frac{\cosh\xi\sin\eta E_\xi + \sinh\xi\cos\eta E_\eta}{\sqrt{\sinh^2\xi + \sin^2\eta}}. \tag{5}$$

The polarization states and the SAMs of the diffraction-free vEHBs generated by six types of dual-modes are all exhibited in Table 1. It can be found that although the six diffraction-free vEHBs have inhomogeneous polarization states in their cross sections, the SAM of the vEHBs generated by the dual-mode of odd $n$ is $1\hbar$ and the SAM of the vEHBs generated by the dual-mode of even $n$ is $-1\hbar$ which fit the counter-clockwise rotation and clockwise rotation of the inhomogeneous polarization states of the vEHBs very well, respectively.

**Table 1.** Polarization states and SAMs of diffraction-free vEHBs.

| Dual-mode excited in the EHF | Rotation direction of the polarization states | SAM |
|---|---|---|
| ${}_{e}HE_{11}$ and ${}_{o}HE_{11}$ ($n=1$) | counter-clockwise | $1\hbar$ |
| ${}_{e}HE_{12}$ and ${}_{o}HE_{12}$ ($n=2$) | clockwise | $-1\hbar$ |
| ${}_{e}HE_{13}$ and ${}_{o}HE_{13}$ ($n=3$) | counter-clockwise | $1\hbar$ |
| ${}_{e}HE_{14}$ and ${}_{o}HE_{14}$ ($n=4$) | clockwise | $-1\hbar$ |
| ${}_{e}HE_{15}$ and ${}_{o}HE_{15}$ ($n=5$) | counter-clockwise | $1\hbar$ |
| ${}_{e}HE_{16}$ and ${}_{o}HE_{16}$ ($n=6$) | clockwise | $-1\hbar$ |

## 5. Conclusions

In this paper, we generate a series of diffraction-free vEHBs by an optical system composed of a short dual-mode EHF and an axicon. Each of vEHBs generated by a dual-mode composed of ${}_{e}HE_{1n}$ mode and ${}_{o}HE_{1n}$ mode ($n = 1, 2, 3, 4, 5, 6$) in the EHF, has a diffraction-free region of more than 1m, and inhomogeneous and periodically-rotated polarization properties. The SAM for each of the diffraction-free vEHBs generated by the dual-mode with odd $n$ is $1\hbar$ and the SAM for each of the vEHBs generated by the dual-mode with even $n$ is $-1\hbar$ which are consistent with their counter-clockwise and clockwise periodically-rotated inhomogeneous polarization states, respectively.

The SAM, as a quantum variable of the photon, offers a degree of freedom that can be exploited in information processing. Since the transfer of SAM always results in the spinning of the particle about its own axis, a blue-detuned diffraction-free vEHB can be used to guide and study the interactions of SAM with cold atoms or molecules, and be applied to nanobiotechnology and biomedicine.[14,15] The cold molecules guided in the vEHB will align in different directions and vary with the guiding distance due to the vEHB's inhomogeneous and space-varying polarization states.[16] And we can obtain a counter-clockwise or clockwise rotation direction by selectively exciting the dual-mode with odd or even subscript $n$. The mechanical behavior of an atomic system interacting with the elliptic symmetric beams can be expected to be interesting.[6] Moreover, in tight-focusing vectorial light beams, the optical spin–orbit interaction may generate three-dimensional spin states rotating around more directions which may offer more degrees of freedom in optical manipulation, spin-independent direction coupling, *etc*.[17–19]

## References


[1] Liu Z R and Jones P H 2016 *J. Opt. Soc. Am. A* **33** 2501
[2] Donato M G, Vasi S, Sayed R, Jones P H, Bonaccorso F, Ferrari A C, Gucciardi P G and Maragò O M 2012 *Opt. Lett.* **37** 3381
[3] Xue Y X, Wang Y S, Zhou S C, Chen H W, Rui G H, Gu B and Zhan Q W 2018 *J. Opt. Soc. Am. A* **35** 953
[4] Westphal V and Hell S W 2005 *Phys. Rev. Lett.* **94** 143903
[5] Wang Z X, Zhang N and Yuan X C 2011 *Opt. Express* **19** 482
[6] Rodríguez-Lara B M and Jáuregui R 2008 *Phys. Rev. A* **78** 033813
[7] Zhou S C, Wang S Y, Chen J, Rui G H and Zhan Q W 2016 *Photon. Res.* **4** B35
[8] Moreno I, Davis J A, Sánchez-López M M, Badham K and Cottrell D M 2015 *Opt. Lett.* **40** 5451
[9] Li H R and Yin J P 2011 *Opt. Lett.* **36** 1755
[10] Li H R and Yin J P 2010 *Chin. Phys. B* **19** 083204
[11] Collins J S A 1970 *J. Opt. Soc. Am.* **60** 1168
[12] Ahluwalia B P S, Cheong W C, Yuan X C, Zhang L S, Tao S H, Bu J and Wang H 2006 *Opt. Lett.* **31** 987
[13] Allen L, Beijersbergen M W, Spreeuw R J C and Woerdman J P 1992 *Phys. Rev. A* **45** 8185
[14] Gao W R and Korotkova O 2007 *Opt. Commun.* **270** 474
[15] Yang Y C, Hou S Y and Deng L Z 2018 *Chin. Phys. B* **27** 053701
[16] Huang Y X, Xu S W and Yang X H 2013 *Chin. Phys. B* **22** 053701
[17] Han L, Liu S, Li P, Zhang Y, Cheng H C and Zhao J L 2018 *Phys. Rev. A* **97** 053802
[18] Shao Z K, Zhu J B, Chen Y J, Zhang Y F and Yu S Y 2018 *Nat. Commun.* **9** 926
[19] Zhang L, Qiu X D, Zeng L W and Chen L X 2019 *Chin. Phys. B* **28** 094202